

# SMARTINTENTNN:

## Towards Smart Contract Intent Detection

Youwei Huang<sup>1,2</sup>, Tao Zhang<sup>1</sup>, Sen Fang<sup>1</sup>, and Youshuai Tan<sup>1</sup>

<sup>1</sup> Macau University of Science and Technology, Macao SAR, China

<sup>2</sup> Institute of Intelligent Computing Technology, Suzhou, CAS, China  
huangyw@iict.ac.cn

**Abstract**—Researchers currently have been focusing on smart contract vulnerability detection, but we find that developers’ intent to write smart contracts is a more noteworthy security concern because smart contracts with malicious intent have caused significant financial loss to users. A more unfortunate fact is that we can only rely on manual audits to check for unfriendly smart contracts. In this paper, we propose SMARTINTENTNN, Smart Contract Intent Neural Network, a deep learning-based tool that aims to automate the process of developers’ intent detection in smart contracts, saving human resources and overhead.

The demo video is available on <https://youtu.be/ho1SMtYm-wI>.

**Index Terms**—Smart Contract, Intent Detection, Automated Software Engineering, Deep Learning

### I. INTRODUCTION

A smart contract is defined as a type of computer program and a transaction protocol to automatically execute, control, or document legally relevant events and actions according to the terms of a contract or an agreement [1]. Generally, users interact with smart contracts by sending transactions to invoke functions. From the perspective of computer programs, current studies on the security of smart contracts mainly focus on the detection of their vulnerabilities or defects. However, as transaction protocols, smart contracts can also be injected with malicious intent by some greedy developers, which may cause potential financial loss.

Fig. 1 gives several samples of unfriendly intent in a real smart contract. We can observe that all functions contain the same modifier: ***onlyOwner***, which means that these *functions* are owned by an account. For instance, if adding the modifier ***onlyOwner*** to the function *changeTax*, a development team can, and only they can, arbitrarily change the tax fee for swapping the assets in a smart contract. Similar to *changeTax*, *teamUpdateLimits* gives the developer the right to modify various limits for transactions. As for the remaining two functions, they express an even worse development intent that allows the owner directly turn on or off the trading function in the smart contract. The mainstream approach to detect smart contracts is manual audits, which are costly and require huge human resources.

To optimize the aforementioned detection process, we present an automated and deep learning-based smart contract intent detection tool: SMARTINTENTNN. It is composed of a universal sentence encoder [2] to generate the contextual

representations (embeddings) [3] of smart contracts, a K-means clustering model [4], [5] to highlight the intent-related representations, and a bidirectional LSTM-based (long-short term memory) [6], [7] multi-label classification network to predict the intent in smart contracts.

```
function changeTax(
    uint8 buyTax,
    uint8 sellTax
) public onlyOwner {
    _buyTax = buyTax;
    _sellTax = sellTax;
}

function setupEnableTrading() public onlyOwner {
    tradingEnabled = true;
}

function setupDisableTrading() public onlyOwner {
    tradingEnabled = false;
}

function teamUpdateLimits(
    uint256 newBalanceLimit,
    uint256 newSellLimit,
    uint256 newBuyLimit
) public onlyOwner {
    balanceLimit = newBalanceLimit;
    sellLimit = newSellLimit;
    buyLimit = newBuyLimit;
}
```

Fig. 1. Examples of a smart contract with malicious intent. BSC address: 0xDDa7f9273a092655a1cF077FF0155d64000ccE2A.

**Our contributions** are summarized as the following points:

- This is the first work to apply deep learning to implement an automated tool for smart contract intent detection;
- We collect an extensible dataset of smart contract source code with ten different categories of intent;
- Our research-used source code, dataset and document are released on <https://gitlab.com/web3se/smartinntent>.

### II. DATASET

As SMARTINTENTNN is implemented on a deep neural network (DNN), we collect a large-scale dataset that contains over 40,000 smart contracts from Binance Smart Chain (BSC) explorer<sup>1</sup> and label them with 10 different types of intent at the *function* code level. We first download open-source smart contracts from the explorer, then we merge those smart contracts in multiple files, and drop the redundant and noisy

<sup>1</sup><https://bscscan.com>

snippets. Finally, we extract the *function* level code snippets in smart contracts.

#### A. Intent Labels

We labelled 10 common categories of intent for the smart contracts in our dataset:

- 1 **Fee** arbitrarily changes transaction fees. The transaction fees paid by users are transferred to the specified wallet addresses.
- 2 **DisableTrading** can directly turn on or off the trading action on a smart contract.
- 3 **Blacklist** restricts the behavior of designated users on smart contracts. This can damage the right of some users to fair and free trade.
- 4 **Reflection** is usually financed by a percentage tax on each transaction. Taxes are redistributed to the holders according to their holding amount. It can attract users to purchase the native tokens without any use case.
- 5 **MaxTX** can limit the maximum number or volume of transactions on a smart contract.
- 6 **Mint** allows issuing new tokens. This issue can be unlimited or artificially controlled.
- 7 **Honeypot** is a smart contract that pretends to leak its funds to a user, provided that the user sends additional funds to it. However, the funds provided by the user will be trapped and retrieved by the honeypot creator [8].
- 8 **Reward** is to reward users with specific crypto assets in the form of dividends to attract users to buy or use the native tokens. These assets may not have value.
- 9 **Rebase**, or elastic, controls the token price by algorithmically adjusting the supply.
- 10 **MaxSell** limits the specified users' selling times or amounts, so to lock their liquidity.

Our label resource is from the StaySafu<sup>2</sup> and the experience of decentralized application developers and auditors.

#### B. Input Extraction

The source code of a smart contract on BSC can be published in two forms. One is the single-file smart contract, whose *imports* are merged by developers before uploading. The other form is a smart contract with multiple files, whose code is uploaded as multiple files. For a multi-file smart contract, we merge all the files into a single document.

The Solidity compiler version specification *pragma*, *import* statements, and *comments* in a smart contract are dropped out. The Solidity compiler version (*pragma*) does not express any developer's intent, and the *code comments* take no impact on the implementation of any intent. Since the external contracts in the *import* statements have been merged in the previous step (multi-file smart contracts), removing the *import* statements will not lose any intent information.

Since a smart contract is a document of computer code, we cannot directly feed an entire smart contract into a neural network. We apply two sets of regular expressions to extract

*contract* level code and *function* level code in smart contracts. The *function* code in a smart contract is what we need to input to our model for training and evaluating, denoted by  $\mathcal{F}$ .

### III. IMPLEMENTATION

The implementation of SMARTINTENTNN can be divided into three primary stages: smart contract embedding, intent highlighting, and multi-label classification learning.

#### A. Smart Contract Embedding

We employ the universal sentence encoder to embed the context of *functions*. We use  $\Phi(\mathcal{F}) : \mathcal{F} \rightarrow \mathbf{f}$  to describe such process, where  $\Phi$  represents the contextual encoder and its input data  $\mathcal{F}$  can be any context of *function*. It outputs a vector  $\mathbf{f}$  which is the embedding of the *function*  $\mathcal{F}$ .

The above operation will be performed on each *function* in a smart contract, and we finally push all the  $\mathbf{f}$  into a matrix  $\mathbf{X}$  to represent an entire smart contract.  $\mathbf{X}$  is an  $n \times m$  matrix where  $n$  equals to the number of *functions* in a smart contract and  $m$  is the embedding dimension.

#### B. Intent Highlight

Although we can directly feed  $\mathbf{X}$  into a DNN, not all *functions* are related to the developer's intent. Thus, we implement an intent highlight module to extract the intent-related *functions* in a smart contract.  $\mathbf{H}(\mathbf{X}) : \mathbf{X} \rightarrow \mathbf{X}'$  describes the highlighting process, where  $\mathbf{H}$  is an unsupervised model and its output is the intent-highlighted data  $\mathbf{X}'$ .

We first train a K-means clustering model to predict the intent strength of each *function*. We randomly select 1,500 smart contracts from our dataset and calculate the frequency of occurrence for each *function*. By our experiments, we find that the frequency of 19 *functions* is greater than 0.75, and we further find these 19 *functions* are commonly used by developers. Through in-depth analysis, we find that these code snippets are usually from public libraries or the code in high-frequency reuse. We thus consider that these *functions* with a high frequency of occurrence express weak intent from the developers. On the contrary, those rarely used *functions* express some specific and strong intent from the developers.

We set the initial  $k$  value as 19, according to the 19 high-frequency *functions*, and set a loop of 80 rounds for K-means training. When comparing the similarity of the two documents, we calculate the *cosine distance* between their embedding vectors [9] [10]. Formula 1 provides a method for calculating the cosine similarity between two *functions* (A and B), that is, the cosine value of  $\mathbf{f}^A$  and  $\mathbf{f}^B$ . Then, we transform cosine similarity to cosine distance by Formula 2.

$$\cos \langle \mathbf{f}^A, \mathbf{f}^B \rangle = \frac{\mathbf{f}^A \cdot \mathbf{f}^B}{\|\mathbf{f}^A\| \|\mathbf{f}^B\|} \quad (1)$$

$$D(\mathbf{f}^A, \mathbf{f}^B) = 1 - \cos \langle \mathbf{f}^A, \mathbf{f}^B \rangle \quad (2)$$

During the training process, the K-means model repeatedly performs the calculation of the cosine distance between the centroids and their within-cluster *function* vectors. The centroids will be updated after each round and the training target

<sup>2</sup><https://www.staysafu.org>

is to minimize the total within-cluster variation (TWCV) for all the clusters. The training is terminated when reaching the maximum iteration limit or the minimum TWCV is no longer significantly reduced. Eventually, we get the proper centroids for K-means and the value  $k$  is reduced to 16. When obtaining the trained K-means model, we can pass any vector  $f_i$  to it for predicting its within-cluster distance. We regard the within-cluster distance as the strength of the intent of a *function*—**The farther the distance, the stronger the intent.**

$$\mathbf{X}' = \text{scale}(\mathbf{X}) \text{ by } \mu f_i \text{ if } D(f_i, c_j) \geq \lambda \quad (3)$$

In Formula 3, we scale  $f_i$  in  $\mathbf{X}$  by the predicted within-cluster distance to generate a new matrix  $\mathbf{X}'$ , where  $i \in \{1, 2, \dots, n\}$ ,  $j \in \{1, 2, \dots, 16\}$ , and  $\lambda = 0.75$  is a threshold of the distance, beyond which,  $f_i$  is scaled by  $\mu = 2$  times.

### C. Multi-label Classification

In this section, we leverage a DNN model for multi-label classification. Our model can be divided into three layers: an input layer, a bidirectional LSTM (BiLSTM) layer, and a multi-label classification layer. We feed the matrix  $\mathbf{X}'$  into the model to train it by minimizing 10 concatenated binary cross entropy losses, according to the 10 labels in Section II.A.

We assume that the input layer accepts a sequence of  $a \times b$  size. The number of *functions* input for each time should be equal to  $a$ . The number of features in each *function* embedding should be equal to  $b$ . The feature number is fixed, hence we do not need to make any change to the columns of  $\mathbf{X}'$ . The only thing we need to ensure is that  $b$  equals to the number of features in  $f_i$ . However, the row size of  $\mathbf{X}'$  is determined by the number of *functions* in each smart contract. There is a situation for  $\mathbf{X}'$ , where the number of its rows may be less than  $a$ . As our input layer is also a masking layer and the masking value is 0, we can pad the absent rows of  $\mathbf{X}'$  with zero vectors.

The second layer is a bidirectional LSTM layer, accepting an  $a \times b$  matrix, which is the output of the previous input layer. Each LSTM layer contains  $a$  memory cells, thus there are a total of  $2a$  cells. In each cell, data is passed and processed through the LSTM input gate, forget gate, and output gate to learn the representation of smart contract semantic context. We set  $h$  hidden units and use a vector  $\mathbf{h}$  to represent the output of a cell. We assume that the forward layer outputs  $\mathbf{h}^f$  and the backward layer outputs  $\mathbf{h}^b$ . Therefore, the final output of the BiLSTM layer is the direct sum of the two outputs through  $\mathbf{h}^f \oplus \mathbf{h}^b$  [11], denoted by  $\mathbf{h}$ .

$$\mathbf{y} = \text{sigmoid}(\mathbf{W}\mathbf{h} + \mathbf{b}) \quad (4)$$

The output of the BiLSTM layer is eventually passed to a multi-label classification dense layer. Formula 4 performs a binary classification on each intent label through a sigmoid function. The shape of weight matrix  $\mathbf{W}$  is  $l \times 2h$ , where  $2h$  is the size of input vector  $\mathbf{h}$  and  $l$  is the number of target labels. Therefore, the final output is a vector  $\mathbf{y} = [y_1, y_2, \dots, y_l]$  and the value of each element in it indicates the probability of one

intent category existing in a smart contract. So far, the intent detection of a smart contract is completed.

## IV. APPLICATION

We utilize *Tensorflow.js* [12] to build SMARTINTENTNN as a website tool so that anyone can easily access it on a browser. Specifically, SMARTINTENTNN contains two major features: intent highlight and intent detection.

### A. Intent Highlight

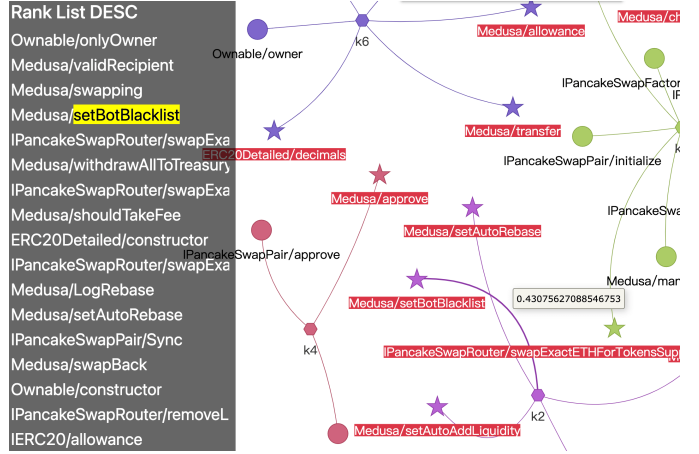


Fig. 2. Example of intent highlight applied on a smart contract. BSC address: 0xE97CBB39487a4B06D9D1dd7F17f7fBBda4c2b9c4.

The intent highlight can help users quickly locate *functions* in smart contracts that contain specific and strong development intent. In Fig. 2, *functions* with strong intent are name-highlighted with red background. Specifically, a hexagon node represents the centroid of its corresponding cluster and the circle node represents a *function* with weak intent while a star represents one with strong intent. When an edge is focused, the distance from the centroid to the *function* is displayed, which represents the strength of the intent. On the left side of the user interface, we list *functions* in a smart contract in descending order of intent from strong to weak.

From Fig. 2, we can observe that there are several *functions* highlighted with red background, e.g., *setBotBlacklist* and *setAutoRebase*, in which really exists some suspicious intent, and they may belong to the intent category of **blacklist** and **rebase** described in Section II.A. Those non-highlighted *functions* are mainly interfaces or libraries, e.g., *functions* in *IPancakeSwapFactory*.

### B. Intent Detection

The intent detection provides a text area for users to type or copy the real smart contract source code and then utilizes SMARTINTENTNN to predict *functions*'s intent in it. Those predicted as high probability intent labels are displayed to users in red background, while the low-probability ones are displayed in green font.

From Fig. 3, we can find that SMARTINTENTNN successfully detected three malicious intent existing in the given smart

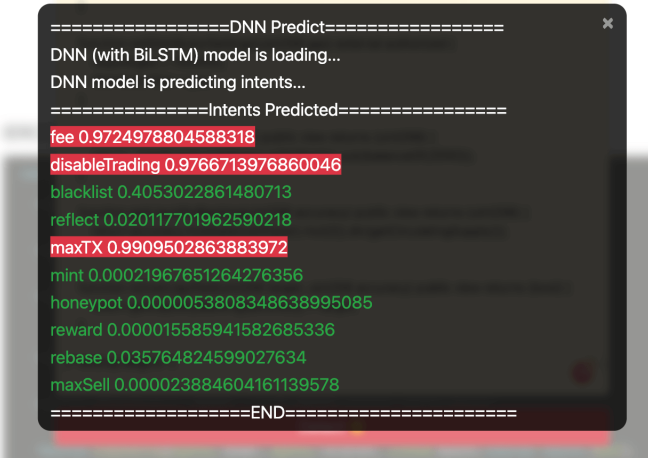


Fig. 3. Example of intent detection applied on a smart contract. BSC address: 0xcF082963E78deAaC10853a220508135505999E6.

contract, i.e., **fee**, **disableTrading**, and **maxTX**. To further verify the output of SMARTINTENTNN, we have checked the smart contract manually and found that these categories of malicious intent really exist in this smart contract. For example, the variable *tradingOpen* in line 403 of the contract controls turning the trading function on or off, which belongs to the **disableTrading** intent. The other two types of intent, **maxTx** and **fee**, are also found in lines 511 and 548 respectively.

## V. EVALUATION

We apply the confusion matrix to evaluate our tool which allows us to measure 4 types of metrics: *recall*, *precision*, *accuracy*, and *f1-score* [13]. We evaluate on 10,000 real smart contracts which do not overlap with our trained dataset. As this is the first work on smart contract intent detection, we have no previous related work to compare. We perform a self-comparison with three baselines, respectively, using a basic LSTM model, a BiLSTM model, and a Convolutional Neural Network model [14] to detect the intent in smart contracts.

TABLE I  
BASELINES COMPARISON

Model	Accuracy	Precision	Recall	F1-score
<b>SMARTINTENTNN</b>				
Scale×2	<b>0.9482</b>	<b>0.8118</b>	<b>0.8308</b>	<b>0.8212</b>
Scale×4	0.9455	0.8380	0.7677	0.8013
Scale×10	0.9435	0.8250	0.7682	0.7956
<b>Other Models</b>				
LSTM	0.9405	0.8126	0.7588	0.7848
BiLSTM	0.9402	0.8033	0.7706	0.7866
CNN	0.9309	0.8395	0.6392	0.7258

The results of evaluation in Table I shows that, of all the baselines and our approach, SMARTINTENTNN with intent highlight scale×2 acquires the highest *f1-score* of 0.8212, the *accuracy* of 0.9482, the *precision* of 0.8118, and the *recall* of 0.8308. Compared with the baselines, *f1-score* is nearly 3%

higher than that of LSTM and BiLSTM, and 9% higher than that of CNN. SMARTINTENTNN performs better than other typical baselines as we use a BiLSTM layer to understand the context of smart contracts both from forward and backward, and further use the intent highlight model to strengthen those code representations with strong intent.

There are two variants of the intent highlight model:  $4\times$ scale ( $\mu = 4$ ) and  $10\times$ scale ( $\mu = 10$ ). All the variants of SMARTINTENTNN can achieve an *f1-score* of more than 0.8 except the model using intent highlight of  $10\times$ scale. It is slightly lower than the best variant of SMARTINTENTNN but still higher than the other models. The reason for this issue is that excessive scale of the embeddings can lead to serious deviation from the actual representation of context.

## VI. CONCLUSION

In this initial work, we present a novel automated tool based on deep learning techniques, namely SMARTINTENTNN, to detect the developers' intent in smart contracts. To implement SMARTINTENTNN, we leverage a universal sentence encoder, a K-means-based intent highlight model, and a DNN integrated with a BiLSTM layer. SMARTINTENTNN is trained on 20,000 and evaluated on 10,000 smart contracts, and it can achieve an *f1-score* of 0.8212.

## REFERENCES

- [1] “Introduction to smart contracts.” [Online]. Available: <https://ethereum.org/en/developers/docs/smart-contracts>
- [2] D. Cer, Y. Yang, S.-y. Kong, N. Hua, N. Limtiaco, R. S. John, N. Constant, M. Guajardo-Cespedes, S. Yuan, C. Tar *et al.*, “Universal sentence encoder,” *arXiv preprint arXiv:1803.11175*, 2018.
- [3] T. Mikolov, I. Sutskever, K. Chen, G. S. Corrado, and J. Dean, “Distributed representations of words and phrases and their compositionality,” *Advances in neural information processing systems*, vol. 26, 2013.
- [4] J. MacQueen, “Classification and analysis of multivariate observations,” in *5th Berkeley Symp. Math. Statist. Probability*, 1967, pp. 281–297.
- [5] K. Krishna and M. N. Murty, “Genetic k-means algorithm,” *IEEE Transactions on Systems, Man, and Cybernetics, Part B (Cybernetics)*, vol. 29, no. 3, pp. 433–439, 1999.
- [6] S. Hochreiter and J. Schmidhuber, “Long short-term memory,” *Neural computation*, vol. 9, no. 8, pp. 1735–1780, 1997.
- [7] I. Sutskever, O. Vinyals, and Q. V. Le, “Sequence to sequence learning with neural networks,” *Advances in neural information processing systems*, vol. 27, 2014.
- [8] C. F. Torres, M. Steichen *et al.*, “The art of the scam: Demystifying honeypots in ethereum smart contracts,” in *28th USENIX Security Symposium (USENIX Security 19)*, 2019, pp. 1591–1607.
- [9] F. Rahutomo, T. Kitasuka, and M. Aritsugi, “Semantic cosine similarity,” in *The 7th international student conference on advanced science and technology ICAST*, vol. 4, no. 1, 2012, p. 1.
- [10] X. Gu, H. Zhang, and S. Kim, “Deep code search,” in *2018 IEEE/ACM 40th International Conference on Software Engineering (ICSE)*. IEEE, 2018, pp. 933–944.
- [11] C. Faith and E. A. Walker, “Direct sum representations of injective modules,” *J. Algebra*, vol. 5, no. 2, pp. 203–221, 1967.
- [12] D. Smilkov, N. Thorat, Y. Assogba, C. Nicholson, N. Kreeger, P. Yu, S. Cai, E. Nielsen, D. Soegel, S. Bileschi *et al.*, “Tensorflow.js: Machine learning for the web and beyond,” *Proceedings of Machine Learning and Systems*, vol. 1, pp. 309–321, 2019.
- [13] S. V. Stehman, “Selecting and interpreting measures of thematic classification accuracy,” *Remote sensing of Environment*, vol. 62, no. 1, pp. 77–89, 1997.
- [14] Y. LeCun, Y. Bengio *et al.*, “Convolutional networks for images, speech, and time series,” *The handbook of brain theory and neural networks*, vol. 3361, no. 10, p. 1995, 1995.